

Article

Detection of Biofilm Formation on Material Surfaces by Ag⁺ Coating

Takeshi Kogo ^{1,*}, Kazufumi Sugi ², Hideyuki Kanematsu ³, Hotaka Kai ⁴, Akiko Ogawa ⁴,
Nobumitsu Hirai ⁴, Toshiyuki Takahashi ⁵ and Takehito Kato ⁶

¹ Department of Materials Science and Engineering, National Institute of Technology (KOSEN), Suzuka College, Shiroko-Cho, Suzuka 510-0294, Japan

² Advanced Engineering Course of Science and Technology for Innovation, National Institute of Technology (KOSEN), Suzuka College, Shiroko-Cho, Suzuka 510-0294, Japan; kougo@suzuka.kosen-ac.jp

³ Cooperative Research & Development Promotion Center, National Institute of Technology (KOSEN), Suzuka College, Shiroko-Cho, Suzuka 510-0294, Japan; kanemats@mse.suzuka-ct.ac.jp

⁴ Department of Chemistry and Biochemistry, National Institute of Technology (KOSEN), Suzuka College, Shiroko-Cho, Suzuka 510-0294, Japan; kai@chem.suzuka-ct.ac.jp (H.K.); ogawa@chem.suzuka-ct.ac.jp (A.O.); hirai@chem.suzuka-ct.ac.jp (N.H.)

⁵ Department of Chemical Science and Engineering, National Institute of Technology (KOSEN), Miyakonojo College, Yoshio-Cho, Miyakonojo 885-8567, Japan; mttaka@cc.miyakonojo-nct.ac.jp

⁶ Department of Mechanical Engineering, National Institute of Technology (KOSEN), Oyama College, 771 Nakakuki, Oyama City 323-0806, Japan; kato_t@oyama-ct.ac.jp

* Correspondence: kougo@mse.suzuka-ct.ac.jp

Abstract: The evaluation of biofilm formation is important, given the ubiquity and problematic nature of biofilms in industrial and medical settings, as well as in everyday life. Basically, biofilms are formed on substrates. Therefore, it is essential to consider the properties of the substrates during biofilm evaluation. The common dye staining method to evaluate biofilm formation requires a short evaluation time and enables the evaluation of a large area of the sample. Furthermore, it can be easily determined visually, and quantitative evaluation is possible by quantifying color adsorption. Meanwhile, the dye staining method has the problem of adsorption even on substrate surfaces where no biofilm has formed. Therefore, in this study, we focused on Ag⁺ reduction reaction to devise a novel biofilm evaluation method. Ag⁺ is highly reductive and selectively reacts with organic substances, such as saccharides, aldehydes, and proteins contained in biofilms, depositing as metallic Ag. First, to simply evaluate biofilm formation, we used a glass substrate as a smooth, transparent, and versatile oxide material. We observed that the amount of Ag deposited on the substrate was increased proportionally to the amount of biofilm formed under light irradiation. Upon comparing the Ag deposition behavior and adsorption behavior of crystal violet, we discovered that for short immersion times in AgNO₃ solution, Ag deposition was insufficient to evaluate the amount of biofilm formation. This result suggests that the Ag reduction reaction is more insensitive than the crystal violet adsorption behavior. The results of the Ag deposition reaction for 24 h showed a similar trend to the crystal violet dye adsorption behavior. However, quantitative biofilm evaluation using the proposed method was difficult because of the Ag⁺ exchange with the alkali metal ions contained in the glass substrate. We addressed this issue by using the basic solution obtained by adding an ammonia solution to aqueous AgNO₃. This can cause Ag⁺ to selectively react with the biofilm, thus enabling a more accurate quantitative evaluation. The optimum was determined at a ratio of distilled water to aqueous ammonia solution of 97:3 by weight. This biofilm was also evaluated for materials other than ceramics (glass substrate): organic material (polyethylene) and metal material (pure iron). In the case of polyethylene, a suitable response and evaluation of biofilm formation was successfully achieved using this method. Meanwhile, in the case of pure iron, a significantly large lumpy deposit of Ag was observed. The likely reason is that Ag precipitation occurred along with the elution of iron ions because of the difference in ionization tendency. It could be concluded that the detection of biofilm formation using this method was effective to evaluate biofilm formation on materials, in which the reduction reaction of [Ag(NH₃)₂]⁺ does not occur. Thus, a simple and relatively quantitative evaluation of biofilms formed on substrates is possible using this method.



Citation: Kogo, T.; Sugi, K.; Kanematsu, H.; Kai, H.; Ogawa, A.; Hirai, N.; Takahashi, T.; Kato, T. Detection of Biofilm Formation on Material Surfaces by Ag⁺ Coating. *Coatings* **2022**, *12*, 1031. <https://doi.org/10.3390/coatings12071031>

Academic Editor: Devis Bellucci

Received: 20 June 2022

Accepted: 14 July 2022

Published: 21 July 2022

Publisher's Note: MDPI stays neutral with regard to jurisdictional claims in published maps and institutional affiliations.



Copyright: © 2022 by the authors. Licensee MDPI, Basel, Switzerland. This article is an open access article distributed under the terms and conditions of the Creative Commons Attribution (CC BY) license (<https://creativecommons.org/licenses/by/4.0/>).

Keywords: biofilm; Ag^+ reduction reaction; biofilm detection; photosensitive

1. Introduction

Biofilms are sticky, gel-like materials produced by microorganisms, such as bacteria [1–3]. Biofilm formation poses problems in the industrial and medical fields, as well as in daily life. For example, mineralization in cooling pipes is caused by biofilm formation [1–3]. Mineral ions, such as Ca^{2+} , Mg^{2+} , and Si^{4+} , usually concentrate in the biofilms where the ions are deposited as hydroxides and carbonates and ultimately clog coolant pipes [4]. Furthermore, biofilms can serve as protective films that inhibit the effectiveness of cleaning agents. Figure 1 shows the mechanism of biofilm formation on a substrate [5–7]. Microorganisms exist as planktonic bacteria in water and the atmosphere. These floating bacteria can adhere to an existing conditioning film present on a substrate and start secreting extracellular substances (EPS). Under favorable conditions, the bacteria multiply and form colonies, and the biofilm grows. Thus, biofilm formation manifests itself on the substrate. Therefore, it is crucial to develop a method to evaluate biofilm formation while also considering the substrate.

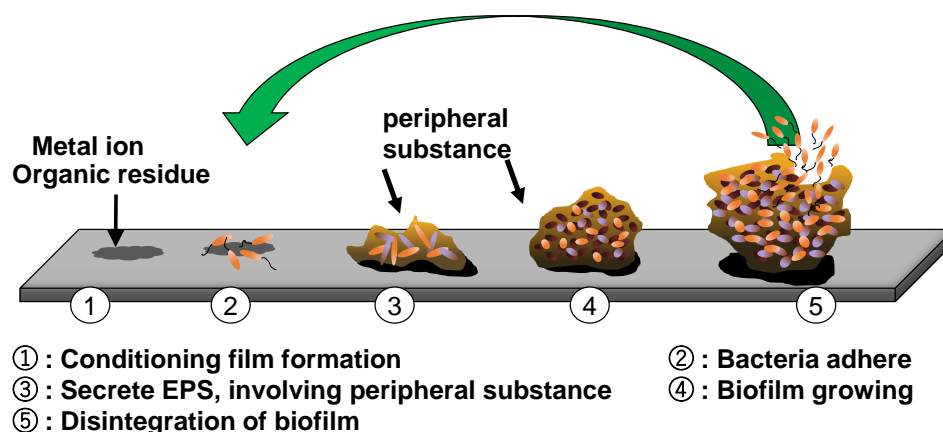


Figure 1. Schematic of biofilm formation.

Several researchers have evaluated biofilm formation [8–36]. For example, confocal microscope, scanning electron microscopy, and atomic force microscopy have been used to directly observe the morphology of biofilms formed on materials [13–17]. Other characterization methods focusing on the organic functional groups contained in biofilms, such as Raman spectroscopy, Fourier transform infrared spectroscopy with attenuated total reflection (FT–IR ATR), and X–ray fluorescence analysis, were employed to identify biofilms [18–22]. Other methods include the electrochemical assessment of biofilm growth using oxygen consumption and quartz crystal measurement methods for in-situ monitoring [23–26]. Many reports were combined with these multiple analyses almost. However, these methods can only analyze localized areas or spots and are often difficult to apply over a wide area. In addition, the equipment is often specialized and expensive, making it difficult to evaluate the methods conveniently.

Dye staining, using dyes, such as crystal violet and alcian blue, is the most popular, simple, and effective biofilm evaluation method for wide areas [27–31]. The dye staining method can be used to evaluate a large area in a short time and can quantitatively evaluate biofilm formation. However, dye absorption on the bare substrate (without the biofilm) is a critical problem encountered during this method. The formation of chemical bonds with the substrates, over-adsorption, and aggregation are possible reasons for this drawback [32–34]. These phenomena are particularly noticeable in the case of several porous metal oxide substrates. For this reason, measures, such as diluting the concentration of the dye solution are taken.

We focused on biofilm-derived organic functional groups. We attempted a biofilm evaluation method that is independent of the substrate properties and employs the Ag^+ reduction reaction, thus contrasting with the dye staining method. Ag^+ is highly reducible and reacts with organic matter, such as saccharides and aldehydes, to precipitate as metallic Ag. This phenomenon is known as the Ag mirror reaction. These organic functional groups are specific to biofilms. In addition, Ag^+ binds well with the amino acid and thiol groups ($-\text{SH}$) contained in the proteins. The reaction of Ag^+ also involves the bacteria contained in the biofilm [35,36]. Therefore, this reaction may be useful in the evaluation of a wide range of biofilm formations, including those that contain bacteria. Furthermore, since the proposed method is a marker technique similar to the dye staining method, it is expected to be simple to evaluate without the need for special and expensive equipment. Table 1 summarizes the characteristics of each analytical evaluation method.

Table 1. The characteristics of each analytical evaluation method.

Analysis Method	Range	Cost	Special Equipment Required	Quantitative/Qualitative
Dye staining	wide	low	not	depend on substrate
FT-IR, Raman	small	high	yes	high reliability
Microscope	small	high	yes	high reliability
Electro Chemical	wide	high	yes	high reliability
Ag deposited method	wide	low	not	this study will reveal

In this study, we proposed that the evaluation of biofilms formed on a metal oxide substrate is possible by utilizing the Ag^+ reduction reaction. The objective is to validate the method on various substrate properties; however, we attempted to first evaluate the method on a commonly used substrate to examine the substrate characteristics. A glass substrate, which is a smooth, transparent, and versatile oxide material, was used as the sample material for ease of biofilm formation evaluation. In addition to the glass substrates, the method was also applied to organic (polyethylene) and metallic materials (pure iron) to clarify their behavior toward biofilm formation.

2. Materials and Methods

2.1. Biofilm Formation Experiment

Soda lime glass plates (Sliding glass, AS ONE, Osaka, Japan) were used as the substrates. Firstly, the glass slides were cut into 2.5×2.5 cm dimensions and washed using ultrasonic treatment with detergent, distilled water, and isopropyl alcohol. The samples were then hydrophilized with aqueous ammonia solution (FUJIFILM Wako Chemicals, Osaka, Japan, Guaranteed Reagent, 28%–30% purity) and hydrogen peroxide solution (FUJIFILM Wako Chemicals, Guaranteed Reagent, 30%–35.5% purity) at 80°C . Polyethylene substrates (Azwan, PEN-101002, Osaka, Japan) were cut into 2.5×2.5 cm dimensions and washed by ultrasonic treatment with distilled water, and isopropyl alcohol. Pure iron substrates (The Nilaco Corporation, purity of 99.5%, Tokyo, Japan) were cut into 2.5×2.5 cm dimensions and washed by ultrasonic treatment with acetone and isopropyl alcohol. Thereafter, they were washed with distilled water and placed in a biofilm reactor that accelerates biofilm formation [20,37,38].

Figure 2 shows a schematic of the biofilm accelerated formation reactor. A strut containing samples fixed inside an acrylic column was inserted, and tap water flowed from the water tank to the inside of the column. Water was passed over a porous metal plate, which then flowed into a water tank such that the area exposed to the atmosphere was increased. At this step, the air was also blown over the porous metal plate, and a large number of microorganisms present in the air were thus mixed in the tank. In these experiments, biofilm formation was evaluated using the aforementioned equipment. Biofilms were formed on the glass substrates by immersing the hydrophilic-treated glass

slides in the biofilm accelerated formation reactor at a water temperature of 30 °C for various immersion times.

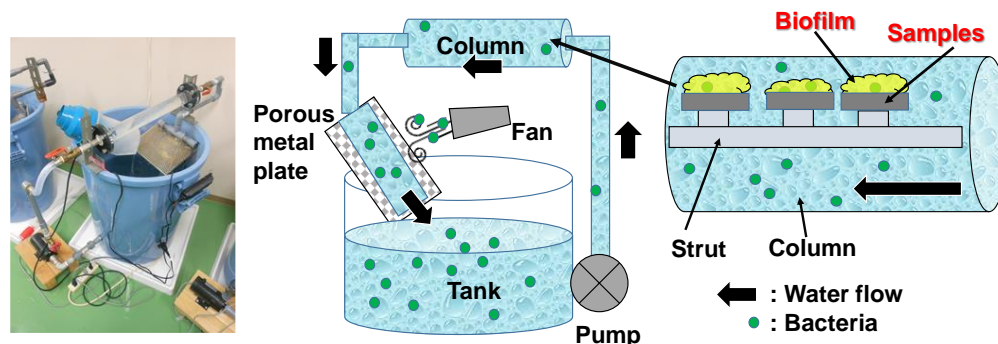


Figure 2. Schematic of the biofilm reactor.

2.2. Evaluation of Biofilm Formation

After the biofilms were formed on the glass slides, the samples were immersed in a 1.0 wt% AgNO_3 (FUJIFILM Wako Chemicals, Osaka, Japan, Guaranteed Reagent, minimum purity of 99.8%) solution. Initially, pure water was used as the solvent. To investigate the effect of light irradiation on the deposited Ag, the samples were immersed in the AgNO_3 solution. These samples were exposed to room light irradiation, while others were covered with aluminum foil (to shield them from the light) for 10 days. Based on the findings from the light irradiation experiment, the experiment involving biofilm formation was performed again in the biofilm accelerated formation reactor.

The biofilm-formed slide glasses were immersed in 1.0 wt% AgNO_3 under ultraviolet irradiation using tabletop Ultra Violet irradiation equipment (ES-27BLB, Sankyo Electric Co., Ltd., Tokyo, Japan) at 25 °C. Crystal violet staining was also conducted for comparison; the biofilm-coated glass substrates were immersed in 0.05 wt% crystal violet solution for 30 min. Biofilm formation was evaluated based on the amount of Ag deposited on the substrate. Subsequently, to inhibit ion exchange, pure water (solvent) was mixed with an ammonia solution (FUJIFILM Wako Chemicals, Osaka, Japan, Guaranteed Reagent, purity of 28%–30%) in ratios of pure water to aqueous ammonia of 100:0 to 95:5 by weight. Following the above experiments, the deposition behavior of Ag on the biofilms formed on the surfaces of glass, pure iron, and polyethylene substrates was evaluated at an optimum concentration of 97:3 by weight of distilled water and ammonia.

The relationship between the amount of biofilm formation and Ag deposition was evaluated visually and via imaging. The Ag-deposited area (black) was extracted and estimated from a photograph using the image analysis software ImageJ (version 1.53K, Wayne Rasband and contributors National Institutes of Health, Bethesda, MD, USA). The images of the crystal violet stained area were also analyzed for comparison with the Ag deposition behavior. Elemental analysis of a small sample area was performed using low-vacuum scanning electron microscopy (SEM; TM-1000, Hitachi, Tokyo, Japan). Components of the biofilm were identified by microscopic laser Raman analysis (NRS-3300, JASCO Corporation, Tokyo, Japan).

3. Results and Discussion

3.1. Investigation of the Ag Deposited by the Effect of Light Irradiation

Figure 3 shows the results of the Raman analysis of the obtained biofilm: (a) biofilm formation after 10 days on the glass substrate, (b) bare-glass substrate. An excitation wavelength of 532.10 nm was used. The result indicated that the peak at approximately 600 cm^{-1} is attributable to Si–O–Si bending vibration in depolymerized structural units, the peak at approximately 800 cm^{-1} can be attributed to Si–O–Si symmetric stretching of bridging oxygen between tetrahedra, and the peak at approximately 1100 cm^{-1} can be attributed to Si–O⁰ and Si–O[−] stretching vibration of Q^n with different n (n = 0,1,2,3,4)

each [39]. However, these peaks were not observed on the biofilm-formed glass substrate, and new peaks appeared. The peak at approximately 960 cm^{-1} is attributable to C-CH₃ rocking; the peak at approximately 1150 cm^{-1} is attributable to band the C-C stretching mode (coupled with C-H in-plane bending), and the peak at approximately 1500 cm^{-1} is attributable to C=C stretching each [21,22]. These peaks had been identified in previous reports and were assumed to be due to multiple microbial groups. The biofilms prepared under these conditions were evaluated for the effect of Ag deposition with and without light irradiation.

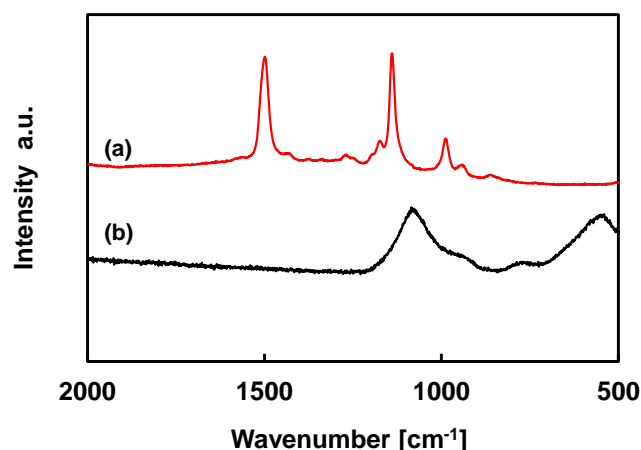


Figure 3. The results of Raman analysis of the obtained biofilm. (a) Biofilm formation after 10 days on glass substrate, (b) Bared—glass substrate.

Figure 4 depicts a comparison of the samples exposed to room light irradiation to those covered with aluminum foil for 10 days. After the first day, Ag deposition was observed on the room light-irradiated sample. In contrast, Ag was deposited slowly on the shielded light sample. This result confirms that the reaction speed depends on the presence or absence of light irradiation, as in the case of silver halide photography. In addition, because no reaction occurred with the experimental equipment (beaker as glass), it was considered that this reaction was reacting with the biofilm formed on the glass substrate. This result indicates that Ag⁺ selectively and qualitatively reacts with the biofilm during the reduction reaction. Moreover, light irradiation plays a major role in determining the reaction rate (indicating photosensitivity).

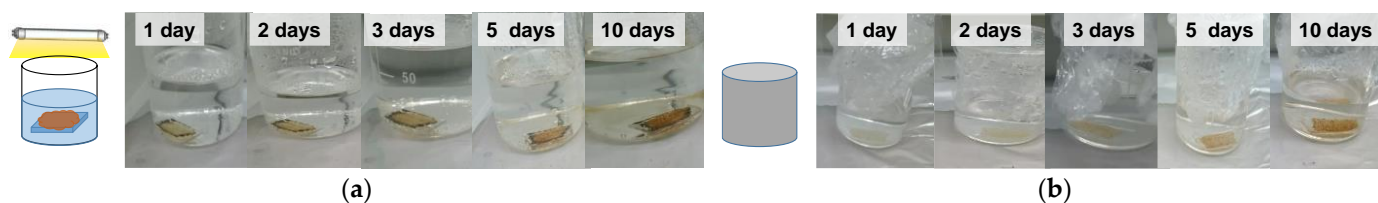


Figure 4. Effect of light irradiation on Ag⁺ reduction. (a) Room light irradiation for 10 days; (b) Shielding light with aluminum foil for 10 days.

3.2. Validation of Ag⁺ Reduction Reaction Method for Quantitative Evaluation of Biofilm

Next, we evaluated the biofilms quantitatively using the Ag⁺ reduction reaction. Figure 5 illustrates the relationship between the amount of biofilm formed and Ag deposited. Ag deposition was confirmed after 0.5 h, indicating that the reaction was significantly promoted by ultraviolet irradiation. It was also confirmed that the amount of deposited Ag increased with the biofilm formation time.

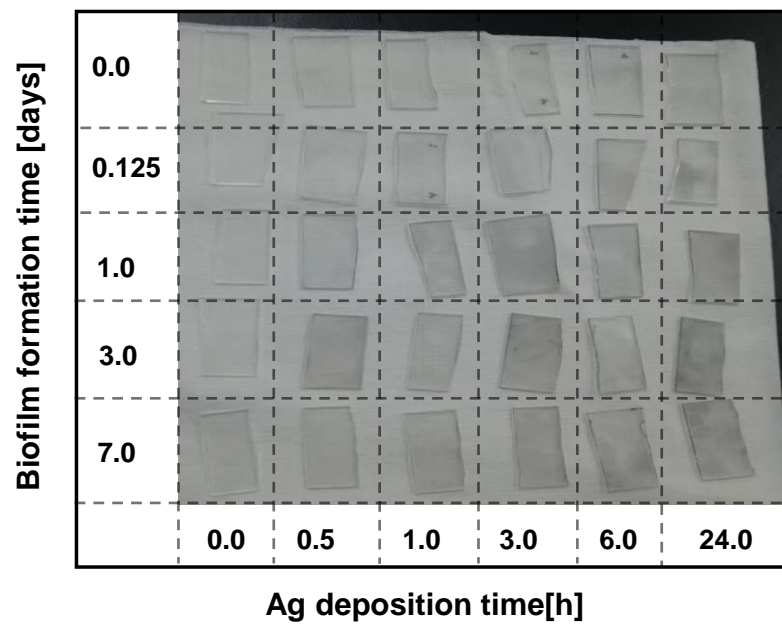


Figure 5. Variation of deposited Ag and biofilm formation with time.

Furthermore, the validity of the Ag deposition method was verified by comparing its adsorption behavior with that in crystal violet dye staining. Figure 6 shows the adsorption of crystal violet dye on the biofilms formed on the glass substrates when immersed in the dye solution for 30 min. The photographs clearly indicate that the amount of dye adsorption increased with increasing biofilm formation time. The amount of dye adsorption was analyzed via image analysis and compared with the Ag deposition sample (Figure 7). Upon comparing the two deposition behaviors, it was observed that when the immersion time of a sample in AgNO_3 solution was short, Ag deposition was insufficient for evaluating the amount of biofilm formed on the substrate. This result indicates that the Ag reduction reaction is more insensitive than the crystal violet adsorption behavior. The results of the Ag deposition reaction for 24.0 h showed a similar trend to the crystal violet dye adsorption behavior.

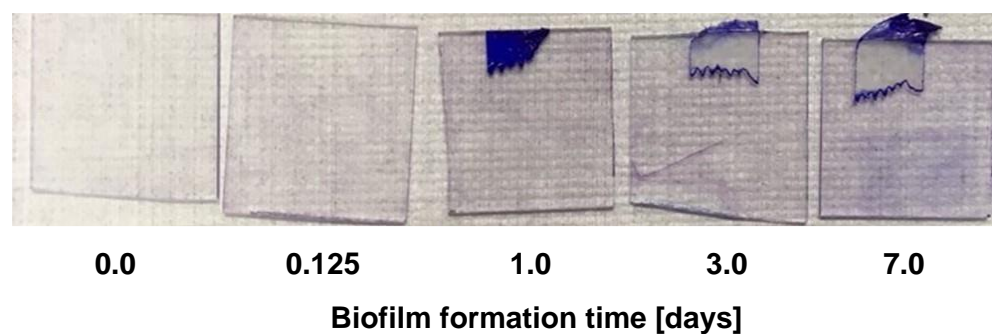


Figure 6. Crystal violet dye staining of biofilm formed on glass substrates.

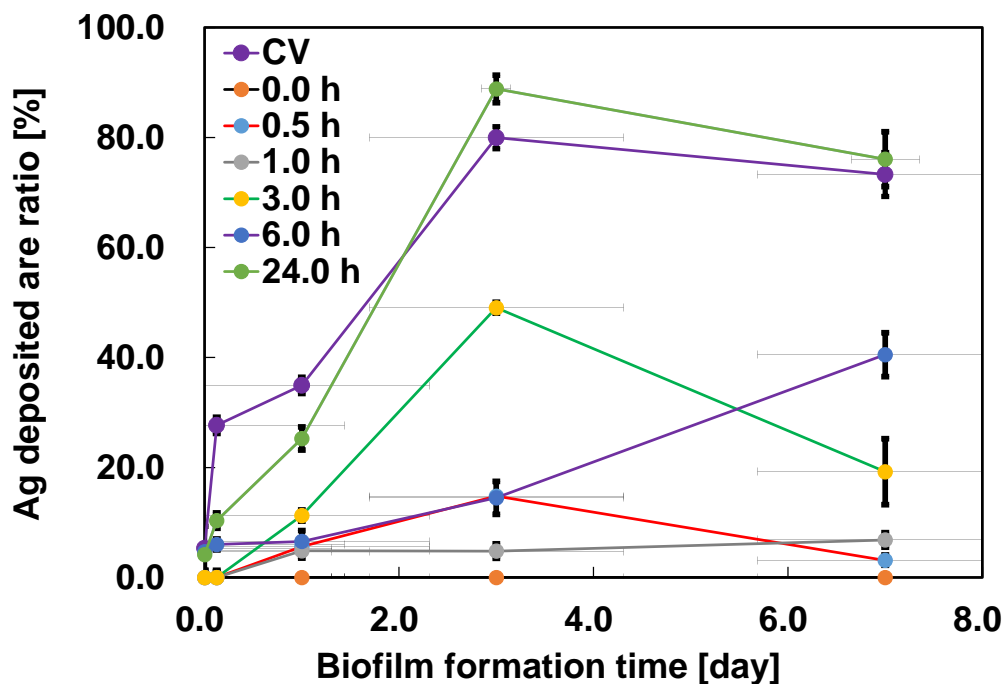


Figure 7. Comparison of Ag and crystal violet dye adsorption behavior.

3.3. Approaches to Suppress ion Exchange Effects

On the other hand, Ag deposition on bare glass (without biofilm) was confirmed following long immersion times over 0.5 h. As a result, elemental analysis was performed on small areas using a low–vacuum SEM. Figure 8 shows the SEM image of the glass substrate with and without the biofilm. The samples containing biofilms show certain deposits (light color). The elemental analysis confirmed that the deposits were composed of Ag. However, even in the absence of biofilm formation, Ag was deposited (Figure 8b). Ag precipitation became more pronounced over time. Upon comparing the morphology of Ag deposited on the biofilms and substrate, it was noted that the former was in an agglomerated state similar to a bacterial colony that grew over time. In contrast, on the substrates that did not experience biofilm formation, Ag was sparsely deposited. Ag precipitation on the glass substrate without biofilm formation was attributed to the ion exchange with the Na⁺ contained in the glass.

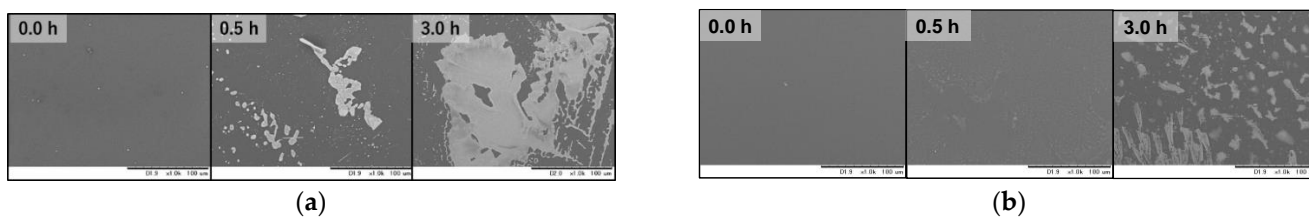


Figure 8. SEM image of the glass substrate immersed in AgNO₃ solution. (a) With biofilm formation; (b) Without biofilm formation.

The glass substrate is basic, and the presence of NO₃⁻ in the solution caused Na⁺ to leach from the glass. Subsequently, negatively charged pores were generated on the glass surface because of the release of Na⁺, and Ag⁺ was reduced on the glass surface. As a result, silver precipitation was considered to have occurred.

To solve this problem, we attempted to suppress the Na⁺ ion exchange by adding an ammonia solution to the AgNO₃ solution. Using this method, Ag⁺ was changed to [Ag(NH₃)₂]⁺, and the pH of the solution became basic. Figure 9 shows the photographs displaying the effect of adding the ammonia solution on the deposition reaction of Ag

on the biofilm. When the amount of added ammonia solution was 98:2 (by weight) or less, black turbidity was observed before the sample was added to the solution. This phenomenon was attributed to the reaction of Ag^+ with OH^- in the basic solution and deposition of Ag_2O . Thus, the reactants did not selectively react with the biofilm on the sample. This phenomenon did not occur when the ratio of the ammonia added to the pure water was 97:3 (by weight) or higher. In this case, Ag precipitation due to the Ag^+ reduction reaction was confirmed.

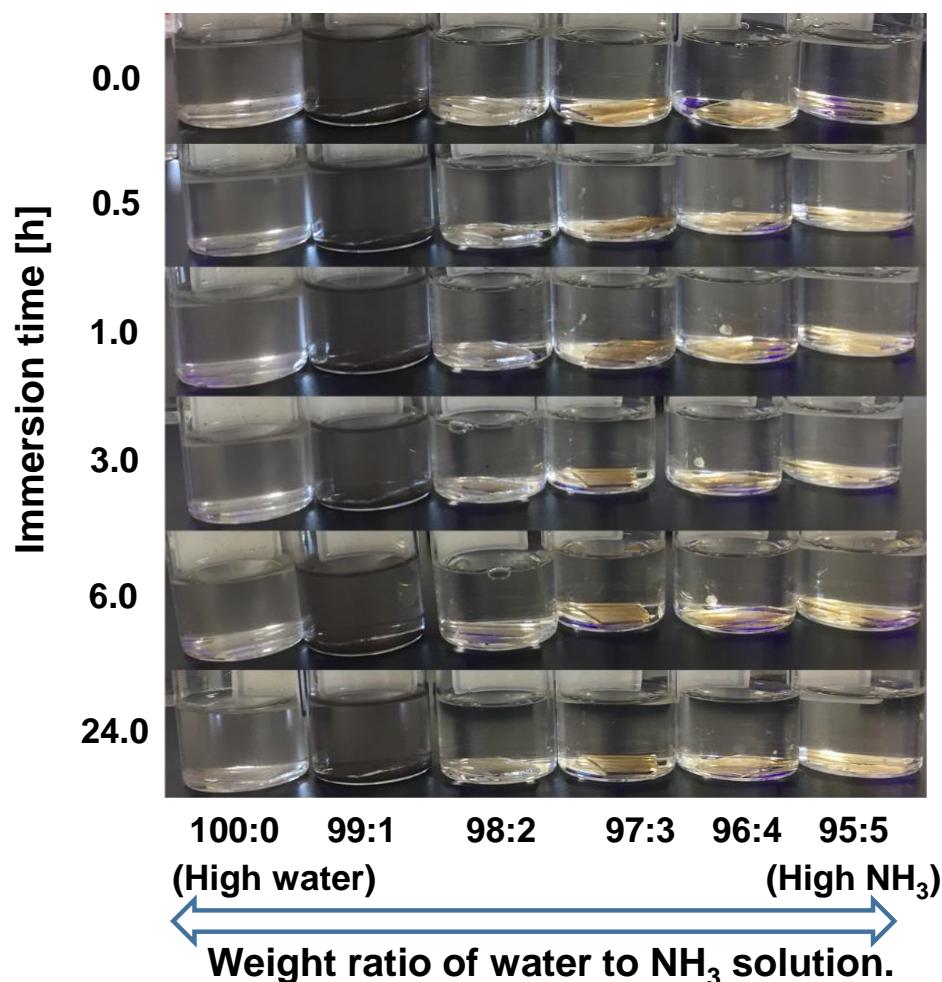


Figure 9. Ag^+ reduction reaction in the presence of NH_3 in solution.

Ag^+ changed to $[\text{Ag}(\text{NH}_3)_2]^+$ in the presence of excess ammonia solution. However, at ratios of 96:4 and 95:5 by weight, the rate of Ag reduction was extremely slow, and it took a long time before Ag precipitation became visible. As a result, it was difficult to quantitatively evaluate the biofilm when the amount of ammonia solution added was low. However, the reaction rate became extremely slow when the ammonia solution concentration was high. In conclusion, the optimal ratio of distilled water to ammonia solution was 97:3 by weight.

In this study, glass substrates were used as the substrate material to facilitate the verification. Further verification of the observation is required in the case of other substrate materials. Figure 10 shows (a) the Ag deposition behavior and (b) crystal violet dye staining results for glass, pure iron, and polyethylene substrates at optimal evaluation concentrations. The results show that the Ag deposition behavior on the polyethylene substrate was excellent and almost consistent with the crystal violet staining behavior on the glass substrate. Meanwhile, significantly large Ag precipitates were observed on the pure iron substrate. This was considered to be due to the ion exchange with $[\text{Ag}(\text{NH}_3)_2]^+$

because of the low ionization tendency of the iron ions. In addition, the weak alkalinity of the aqueous solution was expected to have caused the iron ions from the pure iron to leach out more readily. It was concluded that this experimental method was effective for substrate materials that did not directly contribute to the Ag reduction reaction and where excessive dye adsorption was a problem.

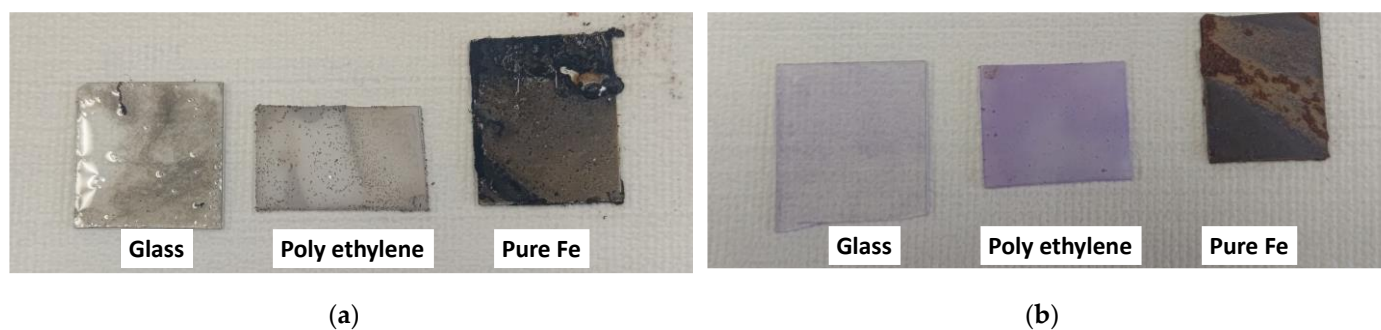


Figure 10. The results of biofilm detection. (a) Ag deposition; (b) Crystal violet dye staining.

The Ag reduction reaction focused on the organic functional groups in the biofilm has a slower reaction rate than that of crystal violet staining. This may be partially because of the environment of the formed biofilm. In addition to the adsorption of Ag^+ onto the biofilm, further Ag^+ reduction reactions are required. The biofilms used in our experiments were formed using several bacteria [32–34]. It is necessary to further examine various types of biofilms as the Ag deposition behavior may be affected by the contents of the reducing materials in the biofilm.

4. Conclusions

In this study, we attempted to use the Ag^+ reduction reaction as a new evaluation method for biofilms. We considered that this method does not require expensive special equipment and can evaluate biofilms as easily as the dye staining method. First, we used a glass substrate as a smooth, transparent, and versatile oxide material to facilitate the evaluation. It was confirmed that the Ag^+ reduction reaction occurred on the biofilm formed on the glass substrate. The reaction rate was significantly accelerated upon light irradiation. Compared to the adsorption behavior of the crystal violet dye, the reaction rate of Ag deposition was slow. It was observed that sufficient reaction with the biofilm required more than 24 h. The trends of Ag deposition and crystal violet adsorption as a result of immersion for 24 h were confirmed to be in good agreement. However, the alkali metal ions contained in the glass slides caused an ion-exchange reaction with Ag^+ , resulting in Ag deposition on the glass substrate, which hindered quantitative evaluation. Therefore, a basic solution was prepared by adding aqueous ammonia to an aqueous AgNO_3 solution. As a result of verification, the optimal condition was observed in a water to aqueous ammonia solution ratio of 97:3 by weight.

In addition, the Ag deposition reaction on the biofilm was also evaluated for polyethylene substrate as the organic material and pure iron substrate as the metal material. It was observed that the Ag deposition behavior on the polyethylene substrate was excellent and nearly matched the staining behavior of crystal violet as well as that of the glass substrate. Meanwhile, significantly large Ag precipitates were observed on the pure iron substrate. This was considered to be due to the ion exchange with $[\text{Ag}(\text{NH}_3)_2]^+$ because of the low ionization tendency of the iron ions. In addition, the weak alkalinity of the aqueous solution is believed to have promoted the elution of iron ions from pure iron.

In conclusion, this experimental method was found to be effective on a substrate material that does not directly contribute to the Ag^+ reduction reaction. This method is simple and inexpensive, this experiment can be further enhanced by evaluating various other materials and biofilms in the future. We also expect its effectiveness to be demon-

strated by combining it with other analytical methods. It is expected that this research and development will facilitate the evaluation of biofilm formation in materials that have been difficult to evaluate by staining, without the use of special and expensive equipment. We expect that expanding to everyday materials, especially porous oxides will enhance research on biofilm formation in conjunction with dye evaluation.

Author Contributions: Conceptualization, T.K. (Takeshi Kogo); experiment of biofilm formation, T.K. (Takeshi Kogo) and K.S.; analysis of picture, T.K. (Takeshi Kogo) and K.S.; observation of SEM and element analysis, T.K. (Takeshi Kogo) and K.S.; consideration for biofilm formation, T.K. (Takeshi Kogo), H.K. (Hideyuki Kanematsu), H.K. (Hotaka Kai), A.O. and N.H.; consideration of Ag⁺ reaction, T.T. and T.K. (Takehito Kato). All authors have read and agreed to the published version of the manuscript.

Funding: This research was supported by the Iron and Steel Institute of Japan, “Creation of New Functions of Slag by Biofilm Coating”.

Institutional Review Board Statement: Not applicable.

Informed Consent Statement: Not applicable.

Data Availability Statement: Not applicable.

Conflicts of Interest: The authors declare no conflict of interest.

References

1. Costerton, J.W.; Lewandowski, Z.; Caldwell, D.E.; Korber, D.R.; Lappin-Scott, H.M. Microbial biofilms. *Annu. Rev. Microbiol.* **1995**, *49*, 711–745. [[CrossRef](#)]
2. Costerton, J.W.; Stewart, P.S.; Greenberg, E.P. Bacterial Biofilms: A Common Cause of Persistent Infections. *Science* **1999**, *284*, 1318–1322. [[CrossRef](#)]
3. Characklis, W.G. Biofilm processes. In *Biofilms*; Characklis, W.G., Marshall, K.C., Eds.; John Wiley & Sons: New York, NY, USA, 1990; pp. 195–231.
4. Kougo, T.; Yamamoto, Y.; Naiki, A.; Ogino, Y.; Kanzaki, T.; Kanematsu, H.; Ikigai, H.; Itoh, H. Proposal for evaluation to Biofilm formation on Metal Oxide in atmospheric exposure type circulation water system. *KOSEN KIYO NIT SUZUKA College* **2013**, *44*, 81–83.
5. Flemming, H.C. Biofouling in water systems-cases, causes, and countermeasures. *Appl. Microbiol. Biotechnol.* **2002**, *59*, 629–640. [[CrossRef](#)]
6. Ofek, I.; Doyle, R.J. *Bacterial Adhesion to Cells and Tissues*; Chapman & Hall: New York, NY, USA, 1994.
7. Lorite, G.S.; Rodrigues, C.M.; de Souza, A.A.; Kranz, C.; Mizaikoff, B.; Cotta, M.A. The role of conditioning film formation and surface chemical changes on *Xylella fastidiosa* adhesion and biofilm evolution. *J. Colloid Interface Sci.* **2011**, *359*, 289–295. [[CrossRef](#)]
8. Larimer, C.; Winder, E.; Jeters, R.; Prowant, M.; Nettleship, I.; Addleman, R.S.; Bonheyo, G.T. A method for rapid quantitative assessment of biofilms with biomolecular staining and image analysis. *Anal. Bioanal. Chem.* **2015**, *408*, 999–1008. [[CrossRef](#)]
9. Birjiniuk, A.; Billings, N.; Nance, E.; Hanes, J.; Ribbeck, K.; Doyle, R.S. Single particle tracking reveals spatial and dynamic organization of the *Escherichia coli* biofilm matrix. *New J. Phys.* **2014**, *17*, 030401.
10. Vyas, N.; Sammons, R.; Addison, O.; Dehghani, H.; Walmsley, A.D. A quantitative method to measure biofilm removal efficiency from complex biomaterial surfaces using SEM and image analysis. *Sci. Rep.* **2016**, *6*, 32694. [[CrossRef](#)]
11. Lee, A.; Park, S.; Yoo, J.; Kang, J.; Lim, J.; Seo, Y.; Kim, B.; Kim, G. Detecting Bacterial Biofilms Using Fluorescence Hyperspectral Imaging and Various Discriminant Analyses. *Sensors* **2021**, *21*, 2213. [[CrossRef](#)]
12. Funari, R.; Shen, Q.A. Detection and Characterization of Bacterial Biofilms and Biofilm-Based Sensors. *ACS Sens.* **2022**, *7*, 347–357. [[CrossRef](#)]
13. Surman, S.; Walker, J.; Goddard, D.; Morton, L.; Keevil, C.; Weaver, W.; Skinner, A.; Hanson, K.; Caldwell, D.; Kurtz, J. Comparison of microscope techniques for the examination of biofilms. *J. Microbiol. Methods* **1996**, *25*, 57–70. [[CrossRef](#)]
14. Pourhajibagher, M.; Bahador, A. Synergistic biocidal effects of metal oxide nanoparticles-assisted ultrasound irradiation: Antimicrobial sonodynamic therapy against *Streptococcus mutans* biofilms. *Photodiagn. Photodyn. Ther.* **2021**, *35*, 102432–102443. [[CrossRef](#)]
15. Wang, J.; Li, G.; Yin, H.; An, T. Bacterial response mechanism during biofilm growth on different metal material substrates: EPS characteristics, oxidative stress and molecular regulatory network analysis. *Environ. Res.* **2020**, *185*, 109451–109461. [[CrossRef](#)]
16. Arenas-Vivo, A.; Amariei, G.; Aguado, S.; Rosal, R.; Horcajada, P. An Ag-loaded photoactive nano-metal organic framework as a promising biofilm treatment. *Acta Biomater.* **2019**, *97*, 490–500. [[CrossRef](#)]
17. Dykas, M.M.; Desai, S.K.; Patra, A.; Motapothula, M.R.; Poddar, K.; Kenney, L.J.; Venkatesan, T. Identification of Biofilm Inhibitors by Screening Combinatorial Libraries of Metal Oxide Thin Films. *ACS Appl. Mater. Interfaces* **2018**, *10*, 12510–12517. [[CrossRef](#)]

18. Kröpfl, K.; Záraya, G.; Vladár, P.; Mages, M.; Ács, É. Study of biofilm formation by total-reflection X-ray fluorescence spectrometry. *Microchem. J.* **2003**, *75*, 133–137. [[CrossRef](#)]
19. Schmitt, J.; Flemming, H.-C. FTIR-spectroscopy in microbial and material analysis. *Int. Biodeterior. Biodegrad.* **1998**, *41*, 1–11. [[CrossRef](#)]
20. Sano, K.; Kanematsu, H.; Kogo, T.; Hirai, N.; Tanaka, T. Corrosion and biofilm for a composite coated iron observed by FTIR-ATR and Raman spectroscopy. *Trans. Inst. Met. Finish.* **2016**, *94*, 139–145. [[CrossRef](#)]
21. Chao, Y.; Zhang, T. Surface-enhanced Raman scattering (SERS) revealing chemical variation during biofilm formation: From initial attachment to mature biofilm. *Anal. Bioanal. Chem.* **2012**, *404*, 1465–1475. [[CrossRef](#)]
22. Horiue, H.; Sasaki, M.; Yoshikawa, Y.; Toyofuku, M.; Shigeto, S. Raman spectroscopic signatures of carotenoids and polyenes enable label-free visualization of microbial distributions within pink biofilms. *Sci. Rep.* **2020**, *10*, 7704–7710. [[CrossRef](#)]
23. Wang, J.; Rong, H.; Zhang, C. Evaluation of the impact of dissolved oxygen concentration on biofilm microbial community in sequencing batch biofilm reactor. *J. Biosci. Bioeng.* **2018**, *125*, 532–542. [[CrossRef](#)]
24. Ripa, R.; Shen, A.Q.; Funari, R. Detecting *Escherichia coli* Biofilm Development Stages on Gold and Titanium by Quartz Crystal Microbalance. *ACS Omega* **2020**, *5*, 2295–2302. [[CrossRef](#)]
25. Kretzschmar, J.; Harnisch, F. Electrochemical impedance spectroscopy on biofilm electrodes—Conclusive or euphonious? *Curr. Opin. Electrochem.* **2021**, *29*, 100757. [[CrossRef](#)]
26. Wilson, C.; Lukowicz, R.; Merchant, S.; Valquier-Flynn, H.; Caballero, J.; Sandoval, J.; Okuom, M.; Huber, C.; Brooks, T.D.; Wilson, E.; et al. Quantitative and Qualitative Assessment Methods for Biofilm Growth: A Mini-review. *Res. Rev. J. Eng. Technol.* **2017**, *6*, 1–42.
27. Christensen, G.D.; Simpson, W.A.; Younger, J.J.; Baddour, L.M.; Barrett, F.F.; Melton, D.M.; Beachey, E.H. Adherence of coagulase-negative staphylococci to plastic tissue culture plates: A quantitative model for the adherence of staphylococci to medical devices. *J. Clin. Microbiol.* **1985**, *22*, 996–1006. [[CrossRef](#)]
28. Pedersen, K. Method for Studying Microbial Biofilms in Flowing-Water Systems. *Appl. Environ. Microbiol.* **1982**, *43*, 6–13. [[CrossRef](#)]
29. Rayner, J.; Veeh, R.; Flood, J. Prevalence of microbial biofilms on selected fresh produce and household surfaces. *Int. J. Food Microbiol.* **2004**, *95*, 29–39. [[CrossRef](#)]
30. Erlandsen, S.L.; Kristich, C.J.; Dunny, G.M.; Wells, C.L. High-resolution Visualization of the Microbial Glycocalyx with Low-voltage Scanning Electron Microscopy: Dependence on Cationic Dyes. *J. Histochem. Cytochem.* **2004**, *52*, 1427–1435. [[CrossRef](#)]
31. Tong, C.; Derek, C. Biofilm formation of benthic diatoms on commercial polyvinylidene fluoride membrane. *Algal Res.* **2021**, *55*, 102260–102271. [[CrossRef](#)]
32. Sun, P.; Hui, C.; Khan, R.A.; Du, J.; Zhang, Q.; Zhao, Y.-H. Efficient removal of crystal violet using Fe₃O₄-coated biochar: The role of the Fe₃O₄ nanoparticles and modeling study their adsorption behavior. *Sci. Rep.* **2015**, *5*, 12638. [[CrossRef](#)]
33. Dil, E.A.; Ghaedi, M.; Ghaedi, A.; Asfaram, A.; Jamshidi, M.; Purkait, M.K. Application of artificial neural network and response surface methodology for the removal of crystal violet by zinc oxide nanorods loaded on activate carbon: Kinetics and equilibrium study. *J. Taiwan Inst. Chem. Eng.* **2016**, *59*, 210–220. [[CrossRef](#)]
34. Brião, G.; Jahn, S.; Foletto, E.; Dotto, G. Adsorption of crystal violet dye onto a mesoporous ZSM-5 zeolite synthesized using chitin as template. *J. Colloid Interface Sci.* **2017**, *508*, 313–322. [[CrossRef](#)]
35. Russell, A.D.; Hugo, W.B. Antimicrobial Activity and Action of Silver. *Prog. Med. Chem.* **1994**, *31*, 351–370.
36. Liao, S.Y.; Read, D.C.; Pugh, W.J.; Furr, J.R.; Russell, A.D. Interaction of silver nitrate with readily identifiable groups: Relationship to the antibacterial action of silver ions. *Lett. Appl. Microbiol.* **1997**, *25*, 279–283. [[CrossRef](#)]
37. Kanematsu, H.; Kudara, H.; Kanesaki, S.; Kogo, T.; Ikigai, H.; Ogawa, A.; Hirai, N. Application of a Loop-Type Laboratory Biofilm Reactor to the Evaluation of Biofilm for Some Metallic Materials and Polymers such as Urinary Stents and Catheters. *Materials* **2016**, *9*, 824. [[CrossRef](#)]
38. Ogawa, A.; Noda, M.; Kanematsu, H.; Sano, K. Application of bacterial 16S rRNA gene analysis to a comparison of the degree of biofilm formation on the surface of metal coated glasses. *Mater. Technol. Adv. Perform. Mater.* **2015**, *30*, B61–B65.
39. Wang, M.; Cheng, J.; Li, M.; He, F. Raman spectra of soda–lime–silicate glass doped with rare earth. *Phys. Rev. B Condens. Matter* **2011**, *406*, 3865–3869. [[CrossRef](#)]